STUDIA UNIVERSITATIS BABEŞ-BOLYAI, CHEMIA, LIV, 4, 2009

DESFERAL EFFECT ON HUMAN ERYTHROCYTE MEMBRANE. AN ATOMIC FORCE MICROSCOPY ANALYSIS

MARIA TOMOAIA-COTISEL[a], DANIELA-VASILICA POP-TOADER[a], ULPIU VLAD ZDRENGHEA[b], GHEORGHE TOMOAIA[c], OSSI HOROVITZ[a] AND AURORA MOCANU[a]

ABSTRACT. The surface topography of erythrocyte membrane was imaged with the atomic force microscope (AFM), operating in tapping mode, and the effect of desferal (deferoxamine mesylate: DFO) at various concentrations on the cell membrane was investigated. The normal (control) human erythrocytes, without DFO, showed a clear concave form. After the incubation of fresh blood with increasing DFO concentrations, from 5×10^{-7} M to 5×10^{-3} M, a progressive increase in both concave depth and surface roughness of erythrocytes were observed. Further, the AFM images indicated that the particles (granules) of the cell surface nanostructure increased with the increasing DFO concentrations. This increase of surface granules is due to the aggregation of lipid nanoparticles and lipid domain formation, induced by DFO. The data are in substantial agreement with our previously published results obtained on lipid membrane models in the presence of DFO. Besides domain formation, the pore formation within human erythrocyte membrane was observed in the presence of desferal.

The DFO effect on lipid membranes might be also associated with the modification of both the conformation and the aggregation of membrane proteins, probably leading to an increased permeability of cell membrane.

Keywords: desferal, domain formation; porous membrane structure; erythrocyte membrane; AFM

INTRODUCTION

The molecular mechanism of the drug interaction with cells and the involvement of interfacial phenomena at the cell membrane are still not well understood, in spite of numerous investigations [1-12]. As a first step, the drugs action presumes that the drug molecules modify the lipid membrane structure [6-12] and thus, they may change the biological membrane properties [5, 9-12].

[a] *Babes-Bolyai University, Faculty of Chemistry and Chemical Engineering, Physical Chemistry Department, 11 Arany J. Str., 400028 Cluj-Napoca, Romania*

[b] *Iuliu Hatieganu University of Medicine and Pharmacy, Psychiatry Department, 43 Babes V. Str., 400012 Cluj-Napoca, Romania*

[c] *Iuliu Hatieganu University of Medicine and Pharmacy, Orthopaedics and Traumatology Department, 47 Mosoiu T. Str., 400132 Cluj-Napoca, Romania. E-mail: mcotisel@chem.ubbcluj.ro*

The objective of the present work is to analyze the effect of a drug, such as desferal, on the structural and topographical characteristics of erythrocyte membrane using atomic force microscopy (AFM). Recently, AFM was used to image the surface of membrane models [13-16] and of cell membranes [17-19]. AFM observations of erythrocyte membranes were used to characterize the membrane structure [20-24] and the AFM images revealed the effect of different organic and inorganic compounds on cellular membrane [25, 26].

Desferal (DFO) or desferrioxamine mesylate is *N*-[5-[3-[(5-aminopentyl)-hydroxycarbamoyl] propionamido] pentyl] -3- [[5-(*N*-hydroxyacetamido)-pentyl] carbamoyl] propionohydroxamic acid monomethanesulfonate (scheme 1). It is a transition metal chelator derived from ferrioxamine B, a sideramine isolated in 1960 from *Streptomyces pilosus*. Since it forms a very stable complex with iron(III), DFO is used for clinically removal of excess iron from blood and tissue [27] and consequently, for the treatment of acute iron poisoning and iron-overload anemia, such as thalassaemia major [28], as well as aluminium poisoning associated with chronic renal dialysis [29].

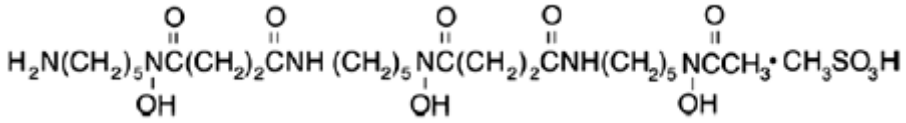

Scheme 1

We have previously investigated the acid and basic properties of desferal [30], and have made a spectroscopic study of this compound and its Fe(III) complex [31, 32]. Since desferal is supposed to act on erythrocyte membrane, we have previously investigated its effects on lipid membrane models, such as lipid monolayers, and determined the domain formation within lipid membrane layers as a function of drug concentration [12].

RESULTS AND DISCUSSION

For this work, we have chosen fresh human blood which offers stable erythrocytes. Erythrocytes samples without or treated with desferal (DFO) are investigated by AFM at room temperature in air.

The erythrocyte cell morphology

AFM images obtained for the whole cell surface morphology of control samples is presented in Figures 1, at two scanned areas of 10 μm x 10 μm and 0.5 μm x 0.5 μm. The AFM images of control samples show that erythrocytes present a concave donut shape with average lateral size.

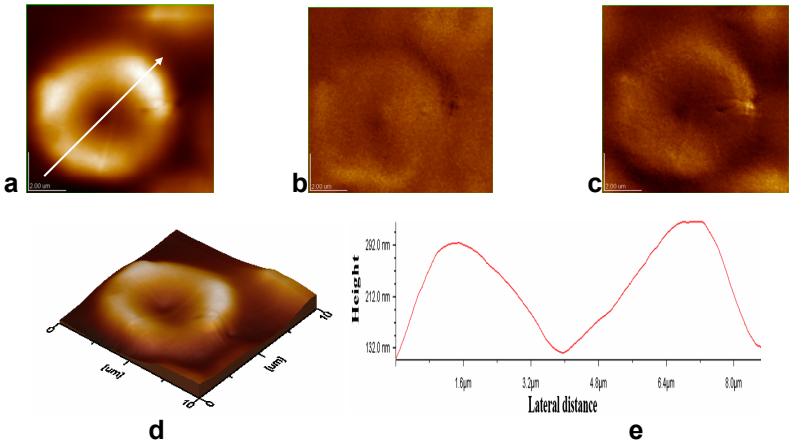

Figure 1A. AFM images of erythrocyte membrane surface, control sample: a) 2D – topography; b) phase image; c) amplitude image; d) 3D-topography; e) profile of the cross section along the arrow in image (a). Scanned area: 10 µm x 10 µm.

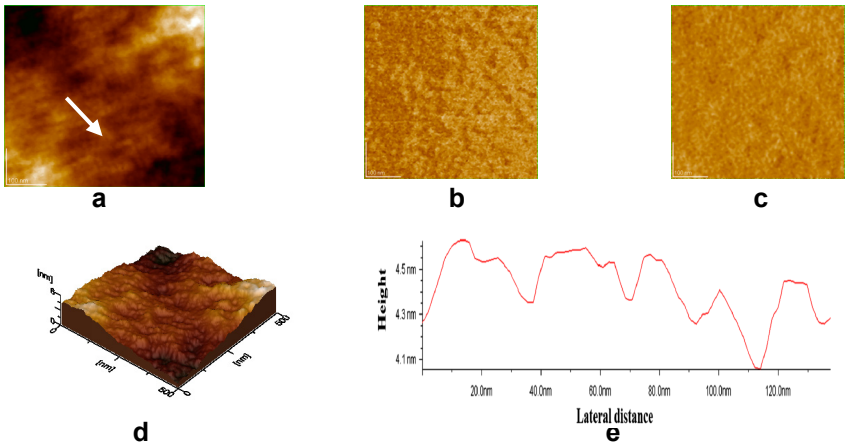

Figure 1B. AFM images of erythrocyte membrane surface, control sample: a) 2D – topography; b) phase image; c) amplitude image; d) 3D-topography; e) profile of the cross section along the arrow in image (a). Scanned area: 0.5 µm x 0.5 µm.

About 8 µm in diameter and nearly 0.14 µm in depth of concave shape (Figure 1A, Table 1). The nanostructure of normal human erythrocytes is featured by closely packed granules or particles with diameter of about 22 nm and almost uniformly distributed (Figure 1B, Table 1).

The granules probably correspond to membrane lipids well packed into the lipid part of the membrane surface in substantial agreement with lipid nanostructure found in monolayer membrane model [16]. These particles might also correspond to membrane protein protruding from the cell surface, mentioned as a probability [20].

The erythrocyte cell morphology in presence of low desferal concentration

Figures 2 and 3 show AFM images of erythrocytes treated with low desferal concentration for two different scanned areas. After mixing of fresh blood with desferal solution the desferal concentration became 5 x 10^{-7} M. The whole surface of erythrocytes is mainly characterized by the same cell shape (Figure 2) as for control sample without DFO (Figure 1A).

The membrane nanostructure in the presence of a low desferal concentration (Figure 3) is only a little different than for control (Figure 1B). The surface roughness, given by root mean square (RMS), is also very similar for these situations at the same scanned area (Table 1).

The erythrocyte cell morphology in presence of medium desferal concentration

The erythrocyte surface morphology is illustrated in Figs 4 and 5, for two different scanned areas, at medium desferal concentration of 5 x 10^{-5} M. AFM images indicate both the cell shape (Figure 4) and membrane surface nanostructures (Figure 5) are perturbed by the presence of desferal at medium concentration.

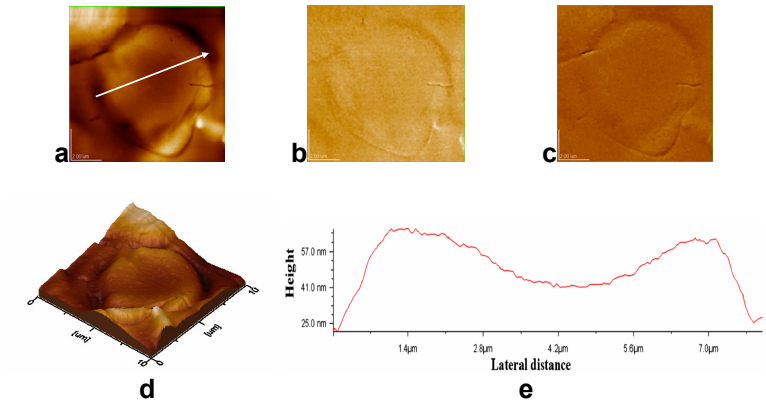

Figure 2. AFM images of erythrocyte membrane surface in the presence of DFO 5 x 10^{-7} M. a) 2D – topography; b) phase image; c) amplitude image; d) 3D-topography; e) profile of the cross section along the arrow in image (a). Scanned area: 10 µm x 10 µm.

Figure 4 presents the AFM images of an erythrocyte at a scanned area of 10 µm x 10 µm. It is clear that the concave form is again preserved as for control sample (Fig 1A), but the concave depth is much higher, to about 340 nm (Figs 4, e). The lateral size of the cell is about 8 or 8.5 µm in diameter.

It is to be noted that in Figure 4, around the cell some NaCl fragments are evidenced, probably formed during the drying process of samples. These small NaCl deposits will not affect the AFM analysis.

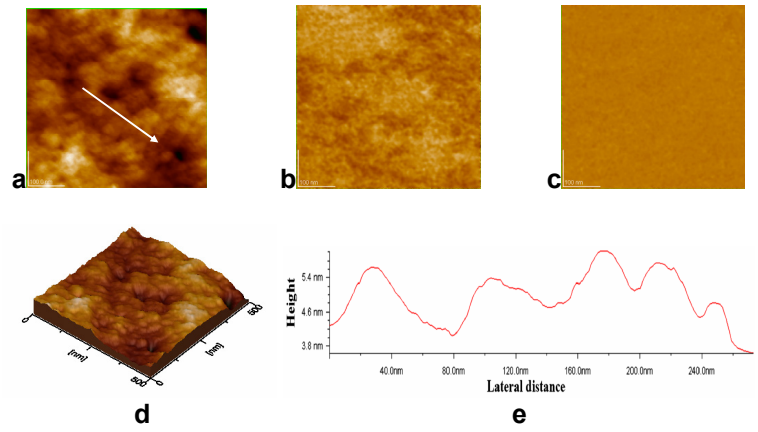

Figure 3. AFM images of erythrocyte membrane surface in the presence of DFO 5 x 10^{-7} M as shown in Figure 2. a) 2D – topography; b) phase image; c) amplitude image; d) 3D-topography; e) profile of the cross section along the arrow in image (a). Scanned area: 0.5 μm x 0.5 μm.

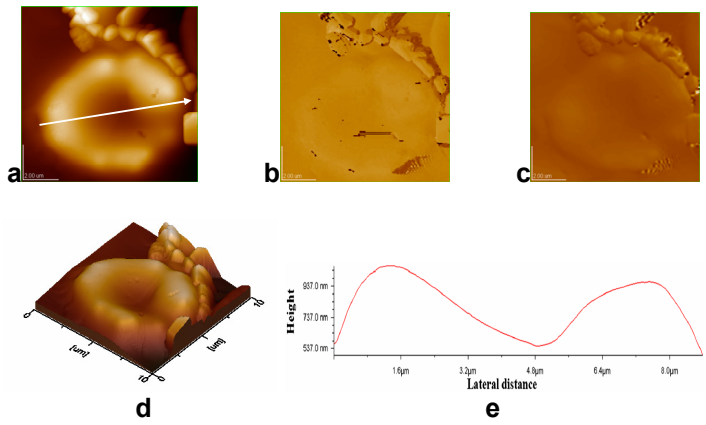

Figure 4. AFM images of erythrocyte membrane surface in the presence of DFO 5 x 10^{-5} M. a) 2D – topography; b) phase image; c) amplitude image; d) 3D-topography; e) profile of the cross section along the arrow in image (a). Scanned area: 10 μm x 10 μm. NaCl crystals were formed during the drying period of the erythrocyte cells on glass surface.

The membrane nanostructure in the presence a medium desferal concentration (Figure 5) is rather different than for control (Figure 1B) or for erythrocytes in presence of low desferal concentration (Figure 3).

The domain formation induced by desferal is well illustrated in Figure 5, particularly in panels b and c. In addition, in Figure 5b it is to be observed a clear tendency to pore formation for this desferal concentration.

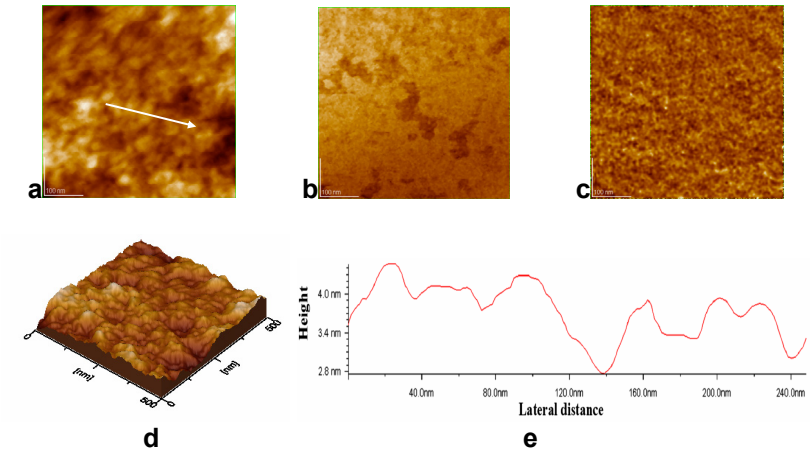

Figure 5. AFM images of erythrocyte membrane surface in the presence of DFO 5 x 10^{-5} M, as shown in Figure 4. a) 2D – topography; b) phase image; c) amplitude image; d) 3D-topography; e) profile of the cross section along the arrow in image (a). Scanned area: 0.5 μm x 0.5 μm.

However, it is to be observed that the membrane nanostructure is relatively uniformed (Figure 5, c and e) and the surface roughness is rather small (Table 1). The granules or surface particles are from about 30 nm to 50 nm (Figure 5 e, and Table 1). From these data, we can suggest a stabilizing effect of desferal on erythrocytes membrane which can be related with the desferal action on sickle cells deformability [33].

The erythrocyte cell morphology in presence of high desferal concentration

The erythrocyte surface morphology is illustrated in Figs 6-10, for four different scanned areas, at high desferal concentration of 5 x 10^{-3} M. AFM images indicate a remarkable change in both cell shape (Figs 6 and 7) and in membrane surface nanostructures (Figs 8-10).

Figure 6 presents the AFM images of several erythrocytes at a scanned area of 15 μm x 15 μm. It is clear that the three cells are somewhat separated from each other, but the cell concave form disappears.

In Figure 7, the AFM images are shown on a single cell (scanned area: 10 μm x 10 μm). Again they show that an erythrocyte is not of concave form, and it is completely different than the control sample (Figure 1A) or than erythrocytes at low (Figure 2) or medium desferal concentration (Figure 4). In other words the concave donut form can no more be identified. This situation can be correlated with a strong interaction of desferal with the cell membrane, leading to the deterioration of the membrane (Figure 6a and Figure 7a).

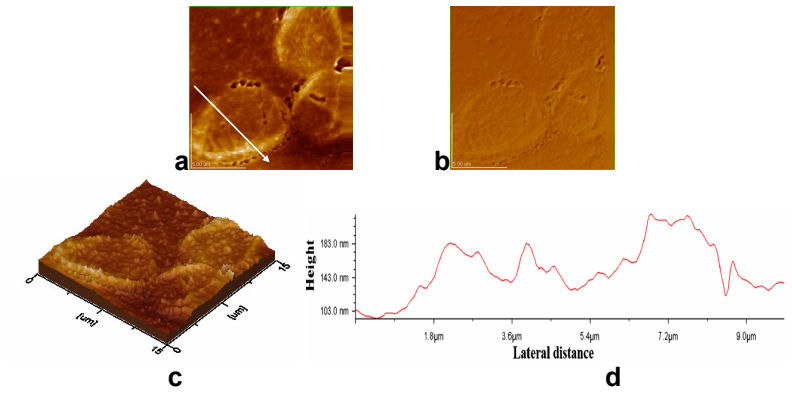

Figure 6. AFM images of erythrocyte membrane surface in the presence of DFO 5 x 10^{-3} M, zone 1. a) 2D – topography; b) amplitude image; c) 3D-topography; d) profile of the cross section along the arrow in image (a). Scanned area: 15 µm x 15 µm.

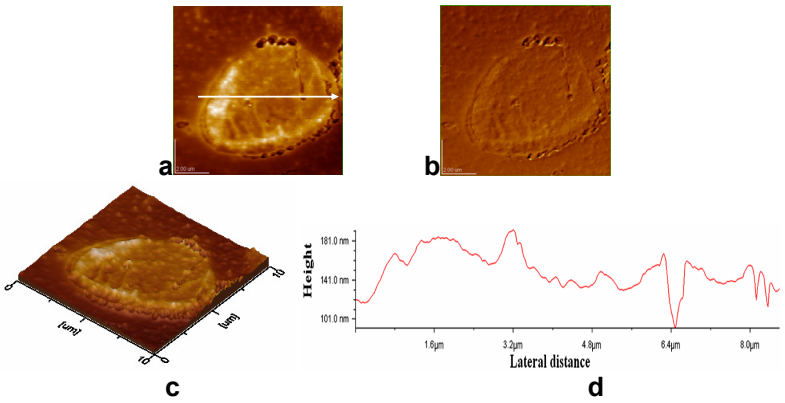

Figure 7. AFM images of erythrocyte membrane surface in the presence of 5 x 10^{-3} M desferal as described in Figure 6. a) 2D – topography; b) amplitude image; c) 3D-topography; d) profile of the cross section along the arrow in image (a). Scanned area: 10 µm x 10 µm.

The membrane nanostructure in the presence of high desferal concentration (Figs. 8 -10) is also much different as that for control sample (Figure 1B) or for erythrocytes in presence of low (Figure 3) or medium desferal concentration (Figure 5).

At this high desferal concentration (5 x 10^{-3} M) the further surface aggregation developed into a long array of aggregated particles and big elongated shaped pores (Figs. 9 and 10). The surface roughness is higher and the granules aggregates are very large (Table 1).

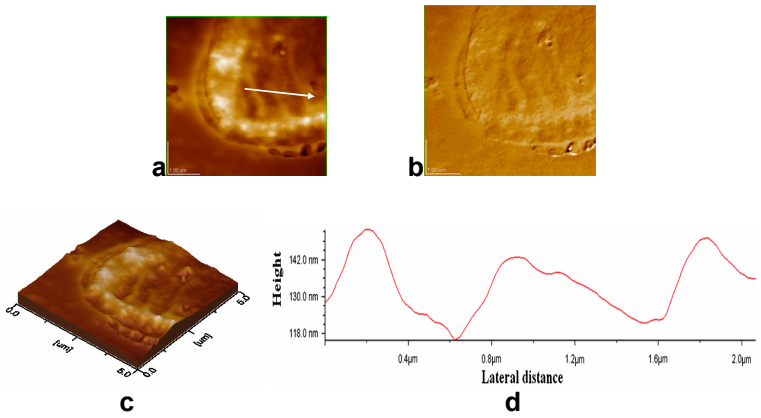

Figure 8. AFM images of erythrocyte membrane surface in the presence of DFO 5 x 10^{-3} M. a) 2D – topography; b) amplitude image; c) 3D-topography; d) profile of the cross section along the arrow in image (a). Scanned area: 5 μm x 5 μm.

Thus, desferal binds to human erythrocyte membranes and induces domain and pore formation on erythrocyte membranes. The domain and pore structures mediated by high desferal concentrations might be responsible for both enhanced surface aggregation of erythrocyte membrane and even perforation.

At low concentration, desferal can only induce the domain structure formation. With a higher DFO concentration, such as 5×10^{-3} M, the further aggregation developed into large pores.

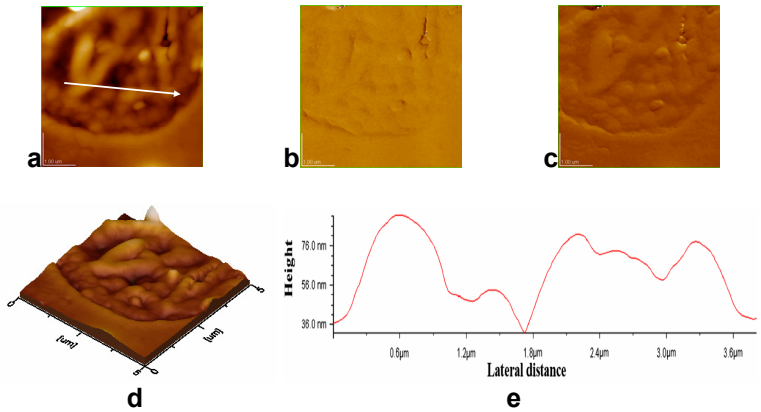

Figure 9. AFM images of erythrocyte surface in the presence of DFO 5 x 10^{-3} M, zone 2. a) 2D – topography; b) phase image; c) amplitude image; d) 3D-topography; e) profile along the arrow in image (a). Scanned area: 5 μm x 5 μm.

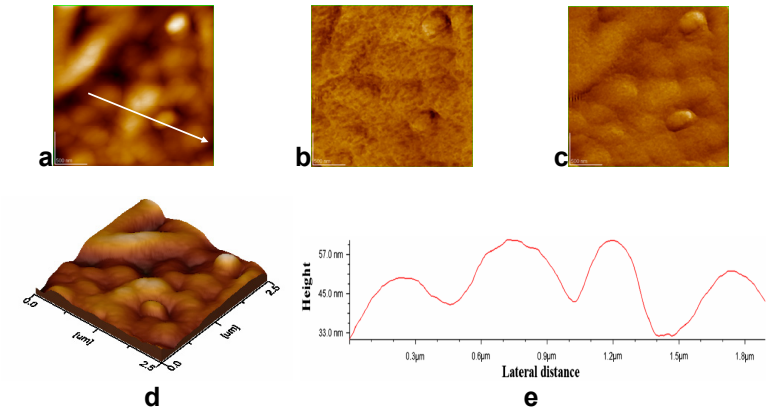

Figure 10. AFM images of erythrocyte membrane surface in the presence of DFO 5 x 10^{-3} M, zone 2. a) 2D – topography; b) phase image; c) amplitude image; d) 3D-topography; e) profile of the cross section along the arrow in image (a). Scanned area: 2.5 µm x 2.5 µm.

The erythrocyte membrane is a mosaic formed from a lipid bilayer with intrinsic and extrinsic proteins. DFO and other drugs may influence the interaction among lipids and proteins and bring changes in the membrane surface structure.

Table 1. Erythrocytes size, concave depth, granules diameter, RMS on scanned areas and on cross profile through the erythrocyte membrane, for fresh blood diluted with 0.15 M NaCl aqueous solution in the 1:1, (v:v), volume ratio, for various desferal (DFO) concentrations.

DFO conc., (M)	Fig.	Scanned areas, (µm x µm)	Cell size (µm)	Concave depth (nm)	Granules (nm)	RMS on scanned areas (nm)	RMS on cross profile (nm)
0	- - 1A 1B	10 x 10 0.5 x 0.5 10 x 10 0.5 x 0.5	8.0 - 8.4 -	135 - 140 -	- 24 - 22	147 1 150 1	99 0.2 101 0.2
5 x 10^{-7}	2 3	10 x 10 0.5 x 0.5	7.7 -	180 -	- 30	170 2	102 0.6
5 x 10^{-5}	- - 4 5	10 x 10 0.5 x 0.5 10 x 10 0.5 x 0.5	8 - 8.5 -	300 - 340 -	- 55 - 50	265 3 274 1	161 2 147 1
5 x 10^{-3}	6 7 8 9 10	15 x 15 10 x 10 5 x 5 5 x 5 2.5 x 2.5	- - - - -	- - - - -	680 600 400 400 230	32 33 25 18 14	32 20 10 16 8

The mechanism of domain and pore formation leading to membrane perforation, provoked by high DFO concentration, could be discussed on the basis of specific interactions among DFO and lipids.

We suggest that the lipid and DFO interactions can lead to the aggregation of membrane lipids and to the coexistence of different lipid and protein phases in the erythrocyte membrane resulting from desferal membrane binding. Of course, the possibility of direct interaction of membrane proteins and desferal can not be eliminated.

The DFO might also alter the interaction of extrinsic proteins with lipid bilayer membrane, again as an effect of the drug binding to the human erythrocytes membranes.

At the same time, desferal molecules penetrated into the lipid membrane can influence the intrinsic membrane proteins and the membrane skeleton.

There might also be a drug distribution into the lipid layers, leading to an increased stability at low DFO concentrations or to a slightly decreased stability of the membrane for medium DFO concentration or even the damage of the erythrocyte membrane at very high DFO concentrations. Domain and pore formation are probably connected to an enhanced permeability of cells in presence of DFO at high concentrations.

Therefore we intend to extend our investigation on erythrocytes in the presence of higher desferal concentrations for a better understanding of desferal effects and potential implications in medical treatment.

CONCLUSIONS

The examination of AFM images on human erythrocytes in the absence and the presence of desferal at different DFO concentrations throw some light on the effect of desferal on cell membranes.

At low DFO concentrations, both the morphology of erythrocyte cells and their membrane nanostructures reveal no a significant difference in comparison with the situation of control sample, erythrocytes without DFO.

At intermediate DFO concentrations, the analysis of AFM images showed that the binding of desferal to erythrocyte membranes led to nanostructured domain formation but at the higher DFO concentration even the pore formation was evidenced.

The domain and pore structures mediated by desferal increased high concentrations might be responsible for both enhanced surface aggregation and the perforation of erythrocyte membrane.

The mechanism of domain and pore formation or the perforation process induced by desferal at its highest concentration used can be discussed on the basis of specific interactions among desferal and the membrane lipids.

These molecular interactions can lead to the aggregation of membrane lipids and to the coexistence of different lipids and proteins phases in erythrocyte membrane resulted from desferal membrane binding.

The possibility of direct interaction of membrane proteins and desferal can also contribute to the erythrocyte membrane changes in the presence of desferal.

EXPERIMENTAL SECTION

Desferal (DFO) of high purity was purchased from Ciba-Geigy, Basle, Switzerland. The DFO concentrations range in aqueous solutions, containing 0.15 M NaCl, was from 5×10^{-7} M to 5×10^{-3} M.

Fresh human blood was used in all experiments. To avoid osmotic pressure modifications, and consequently the swelling of human blood cells, all used aqueous solutions with or without drugs contained 0.15 M NaCl.

Human blood was diluted with 0.15 M NaCl aqueous solution in the 1:1 volume ratio, resulting in the control dispersion. The human blood was also treated with DFO solutions, containing 0.15 M NaCl, in the same 1:1 volume ratio as the control dispersion. The fresh blood was incubated with or without DFO, at room temperature, about 22 ^{o}C, for 30 min.

Then, 10 µL of control and DFO treated blood dispersions were each deposited on optically polished glass plate surface. The residual dispersion was removed with a piece of filter paper placed at the edge of deposited area and the samples were dried in the environmental air conditions.

During the drying process, the control and DFO treated blood samples were covered with a bicker to avoid durst. The dried control samples and DFO treated blood samples were imaged by atomic force microscope, AFM, JEOL 4210.

Atomic force microscopy is a surface imaging technique with a nanometer-scale resolution [13-18]. The cantilevers with a resonance frequency of 250 – 350 kHz were used. Triplicate samples were prepared from each blood sample and at least four separate areas were imaged for every independent sample.

Through this investigation, AFM images were obtained at several drug concentrations in order to examine the effect of desferal on the surface morphology of erythrocytes membrane.

ACKNOWLEDGMENTS

We are grateful for financial support from PN 2, grant no. 41-050.

REFERENCES

1. H. Tsuchiya, M. Mizogami, T. Ueno, K. Takakura, *Inflammopharmacol*., **2007**, *15*, 164.
2. T. Hata, H. Matsuki, S. Kaneshina, *Colloids and Surfaces B*, **2000**, *18*, 41.
3. Z. Leonenko, E. Finot, D. Cramb, *Biochimica et Biophysica Acta,* **2006**, *1758*, 487.

4. H. Matsuki, S. Kaneshina, H. Kamaya, I. Ueda, *Journal of Physical Chemistry B,* **1998**, *102*, 3295.
5. Z. V. Leonenko, D. T. Cramb, *Canadian Journal of Chemistry,* **2004**, *82*, 1128.
6. M. Tomoaia-Cotisel, E. Chifu, A. Mocanu, J. Zsakó, M. Salajan, P.T. Frangopol, *Revue Roumaine de Biochimie,* **1988**, *25* (3), 227.
7. M. Tomoaia-Cotisel, I.W. Levin, *Journal of Physical Chemistry B,* **1997**, *101,* 8477.
8. P. T. Frangopol, D. Mihailescu, *Colloids and Surfaces B,* **2001**, *22*, 3.
9. M. Tomoaia-Cotisel, *Progress in Colloid and Polymer Science*, **1990**, *83,* 155.
10. M. Tomoaia-Cotisel, D. A. Cadenhead, *Langmuir,* **1991**, *7,* 964.
11. B. Asgharian, D. A. Cadenhead, M. Tomoaia-Cotisel, *Langmuir,* **1993**, *9,* 228.
12. M. Tomoaia-Cotisel, A. Mocanu, Gh. Tomoaia, I. Zsako, T. Yupsanis, *Journal of Colloid and Surface Chemistry,* **2001**, *4* (1), 5.
13. M. Tomoaia-Cotisel, "Convergence of Micro-Nano-Biotechnologies, Series in Micro and Nanoengineering", Vol. *9,* Edts. M. Zaharescu, E. Burzo, L. Dumitru, I. Kleps, D. Dascalu, Rom. Academy Press, Bucharest, **2006**, pp. 147-161.
14. K. Hoda, Y. Ikeda, H. Kawasaki, K. Yamada, R. Higuchi, O. Shibata, *Colloids and Surfaces B*, **2006**, *52,* 57.
15. Gh. Tomoaia, M.Tomoaia-Cotisel, A. Mocanu, O. Horovitz, L.-D. Bobos, M. Crisan, I. Petean, *Journal of Optolectronics and Advanced Materials*, **2008**, *10* (4), 961.
16. P. T. Frangopol, D. A. Cadenhead, M. Tomoaia-Cotisel, A. Mocanu, *Studia Universitatis Babes-Bolyai, Chemia*, **2009**, *54* (1), 23.
17. P. C. Zhang, C. Bai, Y. M. Huang, *Scanning Microscopy*, **1995**, *9,* 981.
18. H. J. Butt, E. K. Wolff, S. A. C. Gould, *Journal of Structural Biology,* **1990**, *105*, 54.
19. Y. Cheng, M. Z. Liu, C. I. Bai, *Biochimica et Biophysica Acta,* **1999**, *1421*, 249.
20. X. Y. Zhang, F. H. Chen, P. H. Wei, J. Z. Ni, *Chinese Chem. Letters,* **2006**, *17*, 1105.
21. M. Takeuchi, H. Miyamoto, Y. Sako, H. Komizu, A. Kusumi, *Biophysical Journal*, **1998**, *74*, 2171.
22. S. Yamashina, O. Katsumata. *Journal of Electron Microscopy*, **2000**, *49*, 445.
23. A.H. Swihart, J.M. Mikrut. J.B. Ketterson, R.C. Macdonald, *Journal of Microscopy*, **2001**, *204*, 212.
24. M.S. Ho, F.J. Kuo, Y.S. Lee, *Applied Physics Letters*, **2007**, *91*, 023901.
25. Y. Cheng, M. Liu, R. Li, C. Wang, C. Bai, K. Wang, *Biochimica et Biophysica Acta – Biomembranes,* **1999**, *1421* (2), 249.
26. Y. Cheng, M. Liu, Y. Li, R. Li, C. Bai, K. Wang, *Chinese Science Bulletin*, **2000**, *45*, 426.
27. H. Keberle, *Annals of the New York Academy of Sciences*, **1964**, *119*, 758.
28. W. Banner Jr., T.G. Tong, *Pediatric Clinics of North America*, **1986**, *33,* 393.
29. J.P. Day, P. Ackrill, *Therapeutic Drug Monitoring*, **1993**, *15,* 598.
30. J. Zsako, M. Tomoaia-Cotisel, I. Albu, A. Mocanu, A. Aldea, *Revue Roumaine de Chimie*, **2002**, *47*, 869.
31. O. Cozar, N. Leopold, C. Jelic, L. David, V. Chis, M. Tomoaia-Cotisel, A. Mocanu, R. Grecu, *Studia Universitatis Babes-Bolyai, Physica,* **2004**, *49* (3), 115.
32. O. Cozar, N. Leopold, C. Jelic, V. Chis, L. David, A. Mocanu, and M. Tomoaia-Cotisel, *Journal of Molecular Structure*, **2006**, *788*, 1.
33. M. R. Clark, N. Mohandas, S. B. Shohet, *Journal of Clinical Investigation*, **1980**, *65*, 189.